Heliyon 10 (2024) e40060

Contents lists available at ScienceDirect

Heliyon

journal homepage: www.cell.com/heliyon

Research article

Phosphoproteomics analyses of *Aedes aegypti* fat body reveals blood meal-induced signaling and metabolic pathways

April D. Lopez [a], Tathagata Debnath [a], Matthew Pinch [a,b], Immo A. Hansen [a,*]

[a] New Mexico State University, Las Cruces, NM, 88003, USA
[b] The University of Texas at El Paso, El Paso, TX, 79968, USA

ARTICLE INFO

Keywords:
Phosphoproteomics
Vitellogenesis
Mosquito
Aedes aegypti
Fat-body
Signaling pathway
Blood-meal
Yolk protein precursors

ABSTRACT

The mosquito fat body is the principal source of yolk protein precursors (YPP) during mosquito egg development in female *Aedes aegypti*. To better understand the metabolic and signaling pathways involved in mosquito reproduction, we investigated changes in the mosquito fat body phosphoproteome at multiple time points after a blood meal. Using LC/MS, we identified 3570 phosphorylated proteins containing 14,551 individual phosphorylation sites. We observed protein phosphorylation changes in cellular pathways required for vitellogenesis, as well as proteins involved in primary cellular functions. Specifically, after a blood meal, proteins involved in ribosome synthesis, transcription, translation, and autophagy showed dynamic changes in their phosphorylation patterns. Our results provide new insight into blood meal-induced fat body dynamics and reveal potential proteins that can be targeted for interference with mosquito reproduction. Considering the devastating impact of mosquitoes on human health, worldwide, new approaches to control mosquitoes are urgently needed.

1. Introduction

Aedes aegypti is the vector of major infectious diseases such as dengue, chikungunya, yellow fever, and zika [1]. Mosquitoes spread disease by blood feeding on an infected host and then taking a subsequent blood meal from an uninfected host [2]. Many mosquito species are anautogenous, requiring a vertebrate blood meal for each cycle of egg production [3–5]. Following a blood meal, egg yolk synthesis is initiated in a tissue termed the fat body [5,6].

During the larval phase, the fat body is an active producer of hexametric storage proteins used for metamorphosis [7–9]. In adult mosquitoes, the fat body is located throughout the body with large lobes attached to the abdominal body wall [10]. Fat body tissue is mainly comprised of large polyploid trophocyte cells and few peripheral oenocytes [8,11,12]. The primary functions of the fat body are nutrient storage and protein production for immunity, development, and reproduction [13,14]. Trophocyte cells store nutrients in the form of lipid droplets and protein granules [11,12]. In an earlier study, we have shown that the amount of lipid stores in the fat body decreases shortly after a blood meal and rises again after 24 h [11].

After a blood meal, nutrient and hormone signals induce vitellogenesis [5,15–18]. Vitellogenesis is the process by which yolk precursor proteins (YPP) are synthesized by the fat body and subsequently excreted into the hemolymph and taken up by developing oocytes [19]. In mosquitoes, the fat body is the sole producer of YPPs which are essential nutrients required for embryonic development [5,11]. Post blood meal (PBM), massive quantities of vitellogenin (VG) and other YPPs are synthesized. An earlier RNA-seq

* Corresponding author.
E-mail address: immoh@nmsu.edu (I.A. Hansen).

https://doi.org/10.1016/j.heliyon.2024.e40060
Received 10 July 2024; Received in revised form 29 October 2024; Accepted 31 October 2024
Available online 12 November 2024

analysis revealed YPP-associated genes as the most abundantly expressed transcripts 24 h PBM [7].

As mentioned above, YPP gene expression and translation is regulated via several hormone- and nutrient signaling pathways that have been extensively characterized in earlier studies [5,11,20,21]. Juvenile hormone (JH) plays an early role in ensuring the fat body cells are competent for vitellogenesis [22]. 20-Hydroxy-ecdysone steroid hormone triggers the ecdysone signaling pathway PBM, resulting in amplification of vitellogenin gene expression. The target of rapamycin (TOR) pathway receives signals from amino acid transporters that regulate YPP expression [5]. Insulin-like peptides (ILPs) are essential for direct and indirect regulation of YPP expression in the fat body. Downregulation of ILPs decreases YPP gene expression and egg development [23]. Two types of transcription factors, FOXO and GATA have been shown to essential parts of these signaling cascades [24,25]. Crosstalk between hormone signaling pathways and nutrient signaling pathways are essential for the expression of YPP genes [5,20].

Protein phosphorylation is an important post-translational modification regulatory mechanism of proteins. Phosphate group addition or removal can alter the activity of proteins [26,27]. Phosphoproteomics can give insight to signaling and metabolic pathways that involved in specific biological processes [26,28]. For example, a previous study performed in our lab analyzed the phosphoproteome dynamics of *Aedes aegypti* Malpighian tubules after a blood meal, and revealed altered phosphorylation of a host of proteins associated with osmotic homeostasis, ion transport, and signaling pathways during blood meal processing [29].

To define the phosphoproteome of mosquito vitellogenesis signaling networks [17,20,30], and to reveal key phosphorylation-regulated proteins, we used phosphoproteomics analysis of female *Aedes aegypti* fat body at various time points after a blood meal to investigate dynamic changes within the phosphoproteome. Our results support earlier findings that insulin/FOXO and mTOR signaling pathways are activated after a blood meal and we identified a variety of new signaling pathways that are responsive after a blood meal in the mosquito fat body.

2. Materials and methods

2.1. Mosquito rearing

Aedes aegypti Liverpool strain mosquitoes were used for this study. Eggs were hatched in pans containing 1L of deionized water. Larvae were reared in groups of approximately 250 per pan at 37 °C. Larvae were fed Special Kitty™ cat food pellets *ad libitum* (Walmart Inc., Bentonville, AR). Pupae were separated into dishes and placed into large (30x30 × 30cm) BugDorm-1 cages (MegaView

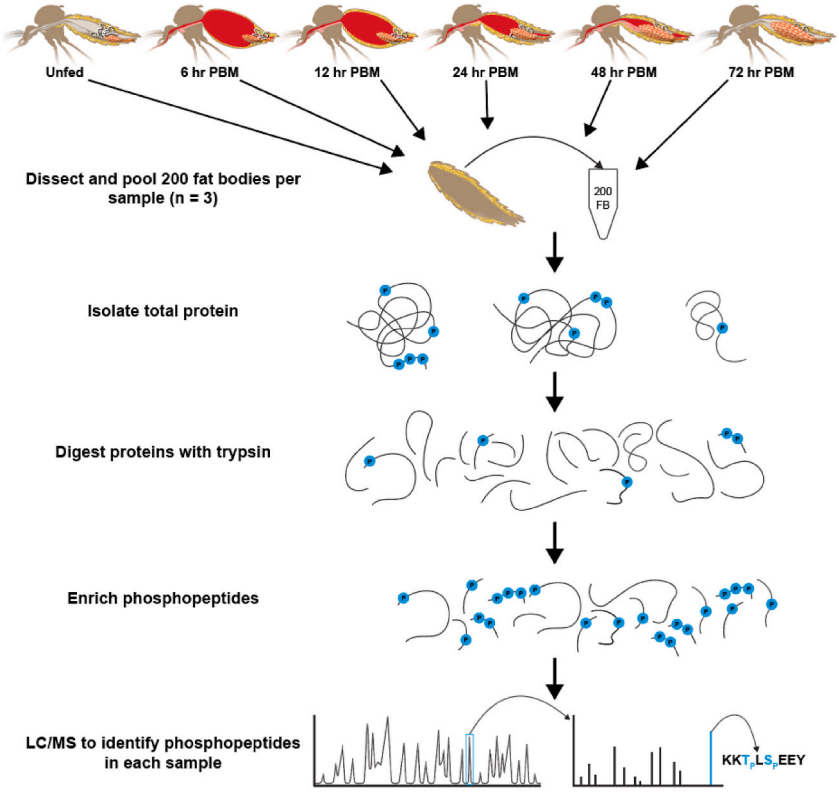

Fig. 1. Experimental flowchart of phospho-proteomics experiment. Protein isolation, phosphopeptide enrichment, and LC/MS analyses were performed by Creative Proteomics (https://ptm.creative-proteomics.com/). Basic mosquito anatomy is illustrated. Mosquito fat bodies, including the abdominal wall, were removed at each time point unfed, 6,12,24,48,72 h post blood meal (PBM). A total of 200 fat bodies were dissected per biological replicate (n = 3). Squiggly lines represent proteins with blue circles as phosphorylation sites.

Science Co., Ltd., Taichung, Taiwan) and allowed to emerge. Adults were kept under standard conditions (27 °C, 80 % humidity, 14hr:10hr light: dark cycle) with unlimited access to 20 % sucrose solution in a 25 mL Erlenmeyer flask with a cotton wick.

2.2. Fat body sampling

One-week post-eclosion, female mosquitoes were fed defibrinated sheep blood (HemoStat Laboratories, Dixon, CA) for 30 min. At 6 h PBM, 12 h PBM, 24 h PBM, 48 h PBM, and 72 h PBM, blood-fed females were anesthetized on ice and their fat bodies were dissected. Using a standard fat body dissection method, abdomens were removed from mosquitoes at each time point PBM, and fat body tissue and adhered cuticle were dissected in modified *Aedes* physiological saline (mAPS) [31]. Three biological samples for each time point (n = 3) were generated by pooling 200 dissected fat bodies in 1 mL of mAPS containing 2 μL each of HALT^{TM} protease inhibitor cocktail (Thermo Scientific, Rockford, IL) and HALT^{TM} phosphatase inhibitor cocktail (Thermo Scientific, Rockford, IL). An additional set of unfed mosquitoes was dissected as a control. All samples were frozen at −80 °C and shipped on dry ice to Creative Proteomics (Shirley, New York) for protein isolation, phosphopeptide enrichment, and phosphoproteomics analysis.

2.3. Phosphoproteomics

Total protein extraction, digestion, phosphopeptide enrichment, and phosphoproteomics analysis (see Fig. 1) were performed by Creative Proteomics (Shirley, New York) as previously described [29]. Briefly, all samples were thawed on ice, and 4 vol of lysis buffer (8M urea, 1 % protease inhibitor, 1 % phosphatase inhibitor) were added. Lysed samples were sonicated using a CL-334 sonicator (Qsonica L.L.C, Newtown, CT) and centrifuged at 12,000×*g* for 10 min at 4 °C to pellet debris. Supernatant was collected from each sample, and total protein content was determined using a BCA assay kit.

Samples were transferred to Microcon devices YM-10 (Millipore, Burlington, MA) and centrifuged at 12,000×*g* and 4 °C for 10 min. Two hundred μL of 50 mM ammonium bicarbonate was added to the concentrated protein, and the process was repeated once. Next, 10 mM DTT was added, and samples were incubated at 56 °C for 1 h to reduce disulfide bonds. 20 mM IAA was added to all samples for 1 h at room temperature in the dark to alkylate cysteine residues. The samples were centrifuged at 12,000×*g* at 4 °C for 10 min and washed once with 50 mM ammonium bicarbonate, and then 100 μL of 50 mM ammonium bicarbonate and free trypsin was added to the samples at a ratio of 1:50. All samples were incubated overnight at 37 °C. The next day, all samples were centrifuged at 12,000×*g* and 4 °C for 10 min and 100 μL of 50 mM ammonium bicarbonate was added. This process was repeated once.

Fe-IMAC beads were prepared by end-over-end rotation for 10 min followed by three washes with 1 mL of wash buffer. Peptide solutions were transferred to the beads, and the whole solutions were rotated for 30 min at room temperature at full speed. After rotation, beads were allowed to settle, and the supernatant was removed. The beads were washed in 1 mL of wash buffer, allowed to settle, and the supernatant was removed. This process was repeated two times for a total of 3 washes. Phosphopeptides were eluted in 50 μL of elution buffer. The supernatant containing eluted phosphopeptides was added to a tube that was previously rinsed with 0.5 mL acetonitrile. 40 μL of 20 % TFA was added to the eluate. The elution was repeated once, and the elution fractions were combined. Eluted phosphopeptides were dried in a speed-Vac and resuspended in 40 μL of 0.1 % FA.

One μg of each sample was loaded into a a Thermo Sceintific™ PepMap™ PepMap C18, 100 Å, 100 μm × 2 cm, 5 μm trapping column followed by a PepMap™ C18, 100 Å, 75 μm × 50 cm, 2 μm analytical column for separation by liquid chromatography. Samples were separated in a two-solvent linear gradient (Solvent A: 0.1 formic acid in water; Solvent B: 0.1 % formic acid in 80 % acetonitrile) with a flow rate of 250 nL/min. The solvent gradient was as follows: first, from 2 % to 8 % Solvent B in 3 min, next from 8 % to 20 % Solvent B in 1 h, then from 20 % to 40 % Solvent B in 23 min, and finally 40 %–90 % Solvent B in 4 min. The MS scan was performed between 300 and 1650 *m/z* with a resolution of 60,000 at 200 *m/z* with an automatic gain control target set to 3e6. The MS/MS scan was operated in Top 20 mode using a resolution of 15,000 at 200 *m/z* with an automatic gain control target of 1e5, normalized collision energy set to 28 %, and an isolation window of 1.4 Th. Charge state exclusion was unassigned, 1, >6 with dynamic exclusion 30 s.

3. Data analysis

3.1. Identification of protein phosphorylation sites

Raw MS files were analyzed against an *Aedes aegypti* protein database using MaxQuant© (1.6.2.14) as previously described [29](see Supplemental Table S1). Entrez Gene IDs and names were assigned to each peptide whose Uniprot ID could be identified.

To assess differential phosphorylation of proteins, fold change and p values were calculated in MS Excel. Principal component analysis (PCA) was used to determine the variability of individual sample groups. PCA analysis and Volcano plots were generated using R programming [32]. In the Volcano plots, the fold-change of individual phosphopeptide amino acid residues for each experimental group was plotted against the unfed group. A fold change less than 0.833(1/1.2) was recorded as down-regulation, while up-regulation was associated with a fold change greater than 1.2. Phosphopeptides with an assigned p-value of less than 0.05 were considered differentially phosphorylated.

3.2. Enrichment analyses

Enrichment analyses were done using Uniprot accession numbers for differentially phosphorylated proteins. All duplicates were

removed manually. Enrichment plots for KEGG analyses and Gene Ontology (GO) analyses were generated in ShinyGO0.08 [33] online tool using default settings. Endomembrane system analysis: protein accession numbers for all differentially abundant phosphoproteins were input in DAVID bioinformatics. All mapped to GO endomembrane system were curated and input as a separate list. The number of protein accession numbers that mapped to each term were input into GraphPad and analyzed as percentages.

3.3. KEGG mapping

Uniprot protein Accession Numbers for all data were entered into DAVID bioinformatics. KEGG Pathway maps were selected based on significant enrichment.

4. Results

4.1. LC/MS analysis

In this data set, we identified a total of 14551 phosphorylated amino acid residues distributed among 3570 proteins, with an average of about 4 phosphorylated amino acid residues per protein (**Supplemental Table 1**).

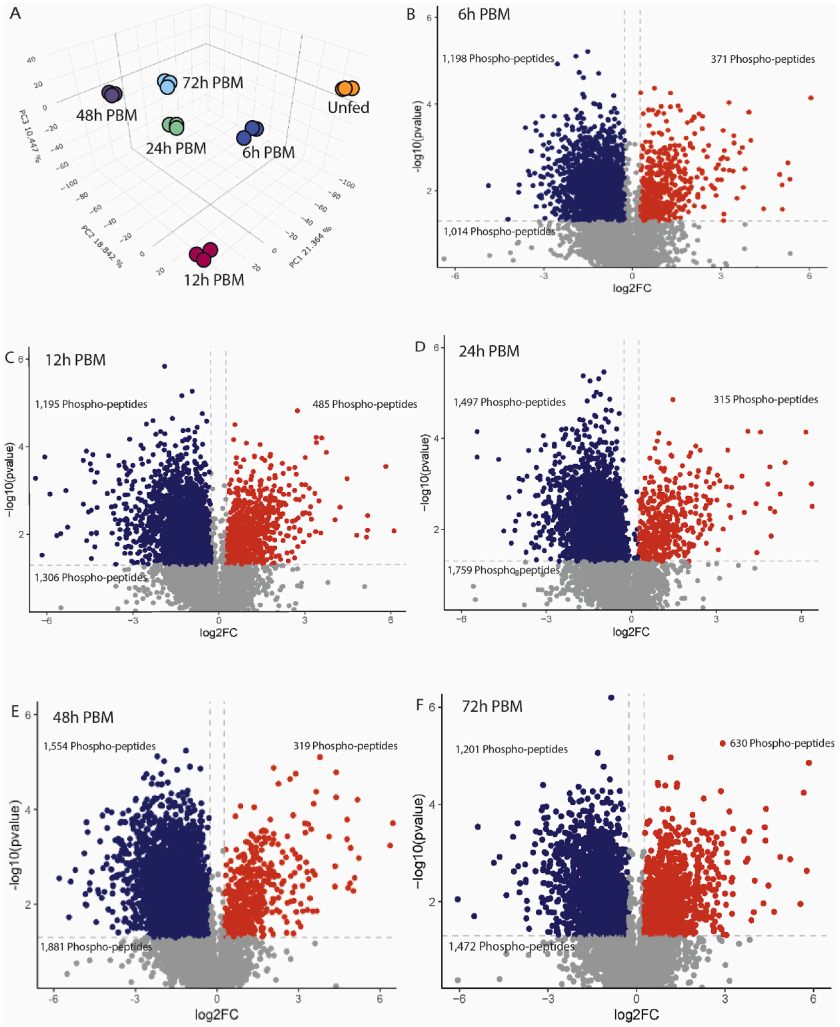

Fig. 2. Statistical analyses of differentially phosphorylated protein residues at sampled time points PBM. (A) Principal component analysis of control showed clear segregation between groups at each time point. (B–F) Volcano plots show significant differentially phosphorylated protein residues at each time point compared to the control (unfed) group. Dotted lines represent fold-change and p-value thresholds. Residues with a significant increase in phosphopeptide abundance are denoted in orange, such with a significant decrease in blue (cut off: FC > 1.2 and FC < 1/1.2, P-value 0.05). (B) Unfed v. 6 hrs PBM, 2583 total phosphopeptides; (C) Unfed v. 12 hrs PBM, 2986 total phosphopeptides; (D) Unfed v. 24hrs PBM, 3571 total phosphopeptides; (E) Unfed v. 48hrs PBM, 3754 total phosphopeptides; (F) Unfed v. 72hrs PBM, 3303 total phosphopeptides.

We used a Principal Component Analysis (Fig. 2A) to compare phosphopeptide abundance sample data for mosquito fat bodies at different time points PBM. There was strong grouping of biological replicates (n = 3) for each time point PBM and very clear segregation between time points PBM.

Differential peptide phosphorylation between unfed and blood-fed female mosquitoes at 6, 12, 24, 48 and 72 h PBM time points are shown in Fig. 2B–F. The fewest differentially abundant phosphopeptides occurred 6 h PBM (Fig. 2B). The number of differentially abundant phosphopeptides increases through 12 h PBM (Fig. 2C) and 24 h PBM (Fig. 2D) with a peak at 48 h PBM (Fig. 2E), before decreasing at 72 h (Fig. 2F) PBM.

4.2. *Enrichment analyses of differentially abundant phosphoproteins*

KEGG analysis identified 25 pathways that were enriched with 20 being significant. The pathways with the highest fold-enrichment in descending order were fatty acid biosynthesis, pentose phosphate pathway, biosynthesis of amino acids, glycolysis/gluconeogenesis, and starch and sucrose metabolism (Fig. 3A). **GO-cellular component** analysis revealed that the proteasome complex, actin cytoskeleton, nucleolus, and ribosome are the cellular components with highest-fold enrichment among all differentially abundant phosphoproteins. (Fig. 3B).

GO-biological process analysis (Fig. 3C) revealed the highest number of phosphoproteins with changed abundance were associated with RNA-processing, translation, and amino acid biosynthesis.

Enrichment Analyses of Phosphoproteins that were differentially increased in abundance KEGG analysis of phosphoproteins that were differentially increased in abundance revealed only two significantly enriched pathways: protein processing in endoplasmic reticulum and nucleocytoplasmic transport (Supplemental Figure 1A). The **GO-cellular component** analysis revealed significant enrichment of the endomembrane system and several different endoplasmic reticulum terms (Supplemental Figure 1B). The **GO-biological processes** analysis revealed nucleotide-containing transport and other related terms as significantly enriched **(Supplemental Figure 1C).**

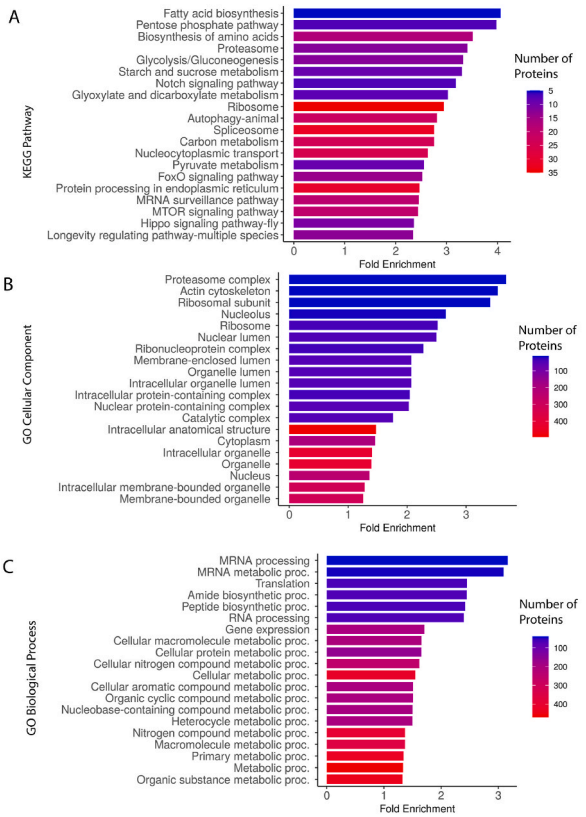

Fig. 3. Enrichment analyses of all differentially abundant proteins. (A–C) Bar plots were generated using ShinyGO. Only significantly enriched pathways are shown (p-adjusted value using false discovery rate (FDR) > 0.05). Terms are sorted from top to bottom by fold enrichment (the percentage of proteins in each pathway divided by the percentage of genes in *Aedes aegypti* genome). The colors of the lines indicate the relative number of proteins identified in each pathway. (A) KEGG pathway enrichment analysis; (B) Gene ontology cellular component enrichment analysis; (C) Gene ontology biological process enrichment analysis.

4.3. Enrichment Analyses of Phosphoproteins that were differentially decreased in abundance

KEGG analysis of phosphopeptides that were differentially decreased in abundance revealed several metabolic and cellular signaling pathways with the highest number of proteins in the ribosome and spliceosome **(Supplemental Figure 2A). GO-cellular component** analysis revealed phosphoproteins with reduced abundance in the nucleus, the proteasome, and the ribosome **(Supplemental Figure 2B). GO-biological processes analysis** revealed decreased phosphoproteins associated with translation and metabolic processes (**Supplemental Figure 2C**).

4.4. Enrichment analyses of differentially abundant phosphoproteins at sampled time points PBM

In general, KEGG pathway analysis showed significant enrichment of phosphoproteins that are part of metabolic and signaling pathways through every time point PBM (Fig. 4A–E). These phosphoproteins are either up- or down-regulated. In the 6, 12, and 24 h PBM time points, the largest number of proteins were mapped to the 'Metabolic pathways' KEGG pathway map (Fig. 4A–C). The GO biological processes termed metabolism, gene expression, RNA processing, and translation were significantly enriched at every time point PBM (Supplemental Fig. 3 A-E). Supplemental Fig. 4 A–E shows the results of the GO cellular component enrichment analysis. The GO molecular function analysis revealed that 'fold enrichment' of phosphoproteins associated with the term 'RNA binding' had the highest significance at every single time point PBM (Supplemental Figure 5). The Uniprot accession numbers of proteins that mapped to each term in our enrichment analysis are listed in **Supplemental Table 1**.

4.5. Top 10 proteins showing maximum change in phosphorylation level

Phosphopeptides with highest and lowest fold-change in abundance at 6, 12, 24, 48, and 72 h PBM compared to the unfed control are shown in **Table 1**. Vitellogenin A1-like (Q177I2) 2036 S was detected as the most abundant phosphopeptide at 6, 12, and 24 h PBM. The phosphopeptides of several ribosomal proteins were detected in the highest fold-change abundance lists at all sampled time points PBM.

Phospho-peptide abundance changes in signaling and metabolic pathways that regulate Cellular-signaling regulation of YPP expression in mosquito fat body.

Fig. 5A–E shows phosphoproteins identified in our dataset. These proteins were chosen, because past studies implicated them in the regulation of vitellogenesis in mosquitoes [5], [34], 35. Shown are the ecdysone-signaling pathway, the mTOR-signaling pathway, the insulin-signaling pathway, and the GCN pathway. We added the Hippo-signaling pathway, because a large number of its proteins were identified (Fig. 5F). Supplemental Table 2-7 depict heatmaps of phosphopeptides that are annotated as part of these signaling pathways. Below is a description of the phosphoproteins associated with these signaling pathways:

Ecdysone Signaling Pathway- We identified seven phosphopeptides across three proteins annotated as part of the Ecdysone Receptor signaling pathway. The nuclear ecdysone receptor (A0A6I8TI42) was detected with two phosphorylation sites. We detected two ecdysone induced proteins-ecdysone- induced protein 74 EF (A0A6I8U2J1) with four phospho-sites and ecdysone-induced protein E75 (A0A1S4FGD0) with one phospho-site (Fig. 5A, Supplemental Table 4).

mTOR Signaling Pathway- We identified 212 phosphopeptides across 29 proteins annotated as part of the mTOR signaling pathway (Fig. 5B–Supplemental Table 2). Most phosphopeptides annotated as part of this pathway did not significantly change in abundance compared to the unfed control (Supplemental Figure 6). KEGG analyses maps show the presence of several nutrient sensors such as the Y + L amino acid transporter, GATOR 1 complex, GATOR 2 complex, and insulin receptor substrate 1 annotated as part of the mTOR pathway (Supplemental Figure 7). Two GATA transcription factors were detected with one phosphorylation site each- GATA 1 (A0A1S4FSA7) and GATA 10 (Q171S6) (Fig. 5B–Supplemental Table 4).

FOXO Signaling Pathways-We identified 134 phosphopeptides across 23 proteins annotated as part of the FOXO signaling pathways (Fig. 5C–Supplemental Table 3). Most phosphopeptides annotated as part of this pathway did not significantly change in abundance compared to the unfed control (**Supplemental Figure 6**). FOXO (A0A6I8TVP2) was detected with 9 phosphorylation sites (Fig. 5C). Insulin receptor protein (Q93105) was detected with one phosphorylation site. (Fig. 5C–Supplemental Table 4), Autophagy Signaling Pathway- We identified 105 phosphopeptides across 24 proteins annotated as part of the autophagy signaling pathway (Fig. 5D–Supplemental Table 5). Six different autophagy-related proteins were detected.

Notch Signaling Pathway- We identified 32 phosphopeptides across 10 different proteins annotated as part of the notch signaling pathway (Fig. 5E–Supplemental Table 6).

Hippo Signaling Pathway- We identified 99 phosphopeptides across 18 different proteins annotated as part of the fly Hippo signaling pathway (Fig. 5F–Supplemental Table 7).

5. Discussion

Mosquito vitellogenesis is activated in the fat body in response to a rise in blood-meal-derived amino acids [36]. Studies on the molecular mechanisms by which the fat body detects and responds to these signals have led to the discovery of several canonical signaling pathways that regulate this process. To gain a more complete picture of the cellular metabolic and signaling pathways and proteins involved, we analyzed the phosphoproteomes of female *Ae. aegypti* fat bodies at different time points after a blood meal. A vitellogenic cycle begins with the uptake of a blood meal and ends with the deposition of fully developed eggs. It takes about 72 h in the yellow fever mosquito *Aedes aegypti* [37]. We isolated and analyzed phosphopeptide abundance in fat bodies of unfed females and at

Table 1
List of the Top-Ten Phospho-peptides with highest and lowest fold-change in abundance compared to the unfed control group. Phospho-peptides are sorted by the 10 phospho-peptides.

Phospho-peptides with highest and lowest fold change at 6 hours PBM

Protein accession #	Position	Amino acid	Found Entrez Description	Time Post Blood Meal						GO biological processes
				Unfed	6hrs	12hrs	24hrs	48hrs	72hrs	
Q177I2	2036	S	vitellogenin-A1-like		156.1	793.72	1857.1	1249	283.45	lipid transport
Q0C740	237	S	40S ribosomal protein S6		66.14	102.47	71.14	88.666	16.058	translation elongation
A0A6I8U478	564	S	breast carcinoma-amplified sequence 3 homolog		40.78	1.255	1.158	1.573	1.584	stress response
Q17M48	48	S	phosphoserine phosphatase		40.49	131.28	83.204	32.265	6.954	organic acid metabolic process
Q0C740	227	S	40S ribosomal protein S6		38.57	28.097	38.124	29.602	5.47	translation elongation
A0A6I8T2W5	867	S	retinoblastoma-like protein 2		33.84	69.141	5.419	1.524	2.961	regulation of transcription of RNA polymerase II promotor
A0A6I8T7N6	1750	T	uncharacterized LOC5576344		33.79	16.346		1.416	3.015	localization
Q0C740	231	S	40S ribosomal protein S6		33.65	35.557	30.458	12.736	9.45	translation elongation
Q0C740	238	S	40S ribosomal protein S6		31.78	36.62	33.282	28.213	8.207	translation elongation
A0A6I8TZB8	237	S	DNA replication factor Cdt1		29.76	24.888		3.073	43.715	DNA replication check point
Q17HX1	44	T	myosin regulatory light chain 2		0.012	0.022	0.004	0.008	1.651	post-embryonic development
Q16WM9	694	S	extended synaptotagmin-2		0.013	0.357	0.357	0.008	0.024	lipid transport
A0A1S4FBU7	75	S	programmed cell death protein 4		0.017	0.609	0.548	0.236	0.009	negative regulation of transcription
Q176C9	197	S	3-phosphoinositide-dependent protein kinase 1		0.034	0.041	0.039	0.032		Protein phosphorylaton
A0A6I8T5E0	7149	T	twitchin		0.035	0.916	0.628	1.624	2.286	cell differentiation
A0A1S4FSP5	771	S	25S rRNA (cytosine-C(5))-methyltransferase nop2		0.037	0.129	0.1			ribosome biogenesis
A0A6I8TZN5	119	S	uncharacterized LOC110679307		0.046		0.766			
Q1HRP3	8	S	40S ribosomal protein S9		0.054	0.296	0.023	0.034	0.183	positive regulation of translational fidelity
A0A1S4FF27	1520	T	transcription elongation factor SPT6		0.055	1.424	0.068	0.473	0.817	transcription from RNA polymerase II promotor
A0A6I8TH48	1193	S	la-related protein 1		0.057	0.073	0.016		0.019	translation regulation

Phospho-peptides with highest and lowest fold change at 12 hours PBM

Protein accession #	Position	Amino acid	Found Entrez Description	Time Post Blood Meal						GO biological processes
				Unfed	6hrs	12hrs	24hrs	48hrs	72hrs	
Q177I2	2033	S	vitellogenin-A1-like			839.18	374.88			
Q177I2	2036	S	vitellogenin-A1-like		156.1	793.72	1857.1	1249	283.45	lipid transport
Q17H62	95	S	extracellular serine/threonine protein CG31145		18.59	135.46	6.856	5.479	13.112	Protein phosphorylaton
Q17M48	48	S	phosphoserine phosphatase		40.49	131.28	83.204	32.265	6.954	alpha-amino acid biosynthetic process
Q0C740	237	S	40S ribosomal protein S6		66.14	102.47	71.14	88.666	16.058	translation elongation
A0A6I8T2W5	867	S	retinoblastoma-like protein 2		33.84	69.141	5.419	1.524	2.961	regulation of transcription of RNA polymerase II promotor
A0A6I8TDG0	751	T	annulin		0.783	62.122	0.689	0.925	57.013	peptide cross-linking
A0A1S4G1S0	803	S	uncharacterized LOC5564282		1.543	60.77	3.381	7.322	2.098	
Q16NF5	122	S	carbohydrate sulfotransferase 5		16.14	56.997	42.875	8.909	1.785	
A0A0P6IVH0	417	S	N/A		18.5	55.163		0.773		
Q16N44	627	S	uncharacterized LOC5575820		0.087	0.002	0.11	0.242	0.754	locomotion
A0A6R5HKD3	4460	S	protein split ends		0.471	0.004	0.265	0.241	0.395	regulation of transcription of RNA polymerase II promotor
A0A6I8U3U1	1068	S	uncharacterized LOC5574048		0.737	0.009	0.508	0.338	0.378	
Q17LZ2	235	T	ribosome biogenesis protein BOP1 homolog			0.009		0.025	0.013	maturation of LSU-rRNA from tricistronic rRNA transcript
A0A1S4FBU7	73	S	programmed cell death protein 4		1.479	0.01	0.28	0.003	0.362	negative regulation of transcription
Q16IW6	143	S	uncharacterized LOC5578143		0.681	0.012	0.478	0.767	1.328	
Q17G16	33	S	endocuticle structural glycoprotein ABD-4		0.483	0.014	0.023		0.051	
A0A6I8TVM1	528	S	eukaryotic translation initiation factor 5B		0.564	0.015	0.552	0.193	0.013	
A0A6I8TJ68	419	S	probable elongation factor 1-delta		0.743	0.015	0.753	1.3	0.374	translational elongation
A0A1S4FKF6	53	S	m7GpppX diphosphatase		0.231	0.017	0.297	0.242	0.462	deadenylation- dependednt capping of nuclear transcribed mRNA's

Phospho-peptides with highest and lowest fold change at 24 hours PBM

Protein accession #	Position	Amino acid	Found Entrez Description	Time Post Blood Meal						GO biological processes
				Unfed	6hrs	12hrs	24hrs	48hrs	72hrs	
Q177I2	2036	S	vitellogenin-A1-like		156.1	793.72	1857.1	1249	283.45	lipid transport
Q177I2	2033	S	vitellogenin-A1-like			839.18	374.88			lipid transport
Q17M48	48	S	phosphoserine phosphatase		40.49	131.28	83.204	32.265	6.954	alpha-amino acid biosynthetic process
Q16YH0	89	S	protein sel-1 homolog 1		2.649	11.791	81.844	82.406	13.657	response to stress, metabolic process
Q0C740	237	S	40S ribosomal protein S6		66.14	102.47	71.14	88.666	16.058	translation elongation
Q16NF5	122	S	carbohydrate sulfotransferase 5		16.14	56.997	42.875	8.909	1.785	
Q0C740	227	S	40S ribosomal protein S6		38.57	28.097	38.124	29.602	5.47	translation elongation
Q0C740	238	S	40S ribosomal protein S6		31.78	36.62	33.282	28.213	8.207	translation elongation
Q176A9	220	Y	serine/arginine-rich splicing factor 1A			28.36	31.764	5.187		
Q0C740	231	S	40S ribosomal protein S6		33.65	35.557	30.458	12.736	9.45	translation elongation
A0A0P6J6M3	258	T	N/A		1.274	0.921	0.001	0.668	0.001	
Q17HX1	44	T	myosin regulatory light chain 2		0.012	0.022	0.004	0.008	1.651	locomotion, post-embryonic development
Q16WU6	373	S	ceramide synthase 6		1.476	0.322	0.009	0.545	0.562	lipid metabolic process
A0A6I8TH48	1193	S	la-related protein 1		0.057	0.073	0.016		0.019	translation regulation
Q16K96	307	Y	serine/threonine-protein phosphatase PP2A		0.374		0.02	0.185	0.451	mitotic cell cycle, cellular protein modification
Q176H6	205	T	phosphoribosyl pyrophosphate synthase-associated protein 2		0.609	0.036	0.021	0.028	0.052	5-phosphoribose-1 diphosphate biosynthetic process
Q1HR36	3	T	14-3-3 protein zeta		0.73	0.696	0.022	1.133	1.018	signal transduction
Q17G16	33	S	endocuticle structural glycoprotein ABD-4		0.483	0.014	0.023		0.051	
Q1HRP3	8	S	40S ribosomal protein S9		0.054	0.296	0.023	0.034	0.183	positive regulation of translational fidelity
A0A6I8T9D2	261	T	protein NDRG3		0.555	0.509	0.025	0.637	0.598	signal transduction

Phospho-peptides with highest and lowest fold change at 48 hours PBM

Protein accession #	Position	Amino acid	Found Entrez Description	Time Post Blood Meal						GO biological processes
				Unfed	6hrs	12hrs	24hrs	48hrs	72hrs	
Q177I2	2036	S	vitellogenin-A1-like		156.1	793.72	1857.1	1249	283.45	lipid transport
Q0C740	237	S	40S ribosomal protein S6		66.14	102.47	71.14	88.666	16.058	translation elongation
Q16YH0	89	S	protein sel-1 homolog 1		2.649	11.791	81.844	82.406	13.657	response to stress, metabolic process
Q16RF4	230	S	paramyosin, long form		5.888	40.172	13.495	61.255	2.037	peptidyl-threonine phosphorylation
Q16YH0	62	S	protein sel-1 homolog 1		1.849	0.763	26.361	45.796	4.317	response to stress, metabolic process
Q16YH0	126	S	protein sel-1 homolog 1		3.42	10.237	29.583	37.142	8.001	response to stress, metabolic process
Q173V7	583	S	sodium-coupled monocarboxylate transporter 1		2.676	7.327	8.099	37.109	54.608	cation transport
A0A6I8TUH8	42	T	extracellular matrix-binding protein ebh		1.425	2.434	0.917	36.111	9.433	phosphorous metabolic process
A0A6I8TRZ3	210	S	glycerophosphocholine phosphodiesterase GPCPD1		4.029	1.912	21.07	35.852	13.744	lipid metabolic process
A0A0P6JSH2	324	S	N/A					33.31	6.132	
A0A1S4FBU7	73	S	programmed cell death protein 4		1.479	0.01	0.28	0.003	0.367	negative regulation of transcription
Q17HX1	44	T	myosin regulatory light chain 2		0.012	0.022	0.004	0.008	1.651	locomotion, post-embryonic development
Q16WM9	694	S	extended synaptotagmin-2		0.013	0.357	0.357	0.008	0.024	lipid transport
A0A6I8T6Q9	955	T	PHD and RING finger domain-containing protein 1		1.542	1.546		0.016	1.011	regulation of macromolecule metabolic process
Q16RF4	232	S	paramyosin, long form		0.187	1.269		0.017	1.438	peptidyl-threonine phosphorylation
Q179R4	558	S	uncharacterized LOC5579827		0.574	0.329	0.087	0.018	0.035	regulation of transcription of RNA polymerase II promotor
Q16NK4	316	S	protein hairy		0.287	0.236	0.05	0.02	0.268	regulation of transcrip[tion from RNA polymerase II promotor
A0A6I8T5E0	7151	T	twitchin		0.57	0.712	0.466	0.027	0.05	Protein phosphorylaton
A0A6I8TH48	954	T	la-related protein 1		0.41	0.196	0.347	0.025		regulation of translation
Q179R4	554	S	uncharacterized LOC5579827		0.526	0.432	0.119	0.024	0.08	regulation of transcription of RNA polymerase II promotor

Phospho-peptides with highest and lowest fold change at 72 hours PBM

Protein accession #	Position	Amino acid	Found Entrez Description	Time Post Blood Meal						GO biological processes
				Unfed	6hrs	12hrs	24hrs	48hrs	72hrs	
Q177I2	2036	S	vitellogenin-A1-like		156.1	793.72	1857.1	1249	283.45	lipid transport
Q16ZI7	49	S	uncharacterized LOC5570231						279.73	protein binding
Q8WRS8	779	S	ribonucleoside-diphosphate reductase large subunit-like		0.938	1.608	0.919	0.737	57.332	DNA replication
A0A6I8TDG0	751	T	annulin		0.783	62.122	0.689	0.925	57.013	peptide cross-linking
Q16PS9	228	S	uncharacterized LOC5574939			1.075			54.613	
Q173V7	583	S	sodium-coupled monocarboxylate transporter 1		2.676	7.327	8.099	37.109	54.608	sodium ion transport
Q8WRS8	802	S	ribonucleoside-diphosphate reductase large subunit-like		1.611	1.862	1.743	1.343	50.791	DNA replication
A0A6I8TN35	309	T	CCR4-NOT transcription complex subunit 3		0.916	0.602	0.629		47.045	nuclear-transcribed mRNA ploy(A) tail shortening
A0A6I8TER3	2209	S	titin				4.756	5.038	46.828	
A0A6I8TZB8	237	S	DNA replication factor Cdt1		29.26	24.888		3.073	43.715	DNA replication check point
A0A0P6J6M3	258	T	N/A		1.274	0.921	0.001	0.668	0.001	
A0A6I8TVM1	530	S	eukaryotic translation initiation factor 5B		0.615	0.038	0.652	0.229	0.004	translation initiation factor activity
A0A1S4FBU7	75	S	programmed cell death protein 4		0.017	0.609	0.548	0.236	0.009	negatice regulation of transcription
Q17LZ2	235	T	ribosome biogenesis protein BOP1 homolog			0.009		0.025	0.013	maturation of LSU-rRNA from tricistronic rRNA transcript
A0A6I8TVM1	528	S	eukaryotic translation initiation factor 5B		0.564	0.015	0.552	0.193	0.013	
A0A1S4F8D1	536	S	E3 ubiquitin-protein ligase HRD1		1.046	0.66	2.561	1.258	0.019	protein ubiquitination
A0A6I8TV40	634	S	collagen alpha-1(XVIII) chain						0.015	anatomical structure development
A0A6I8TH48	1193	S	la-related protein 1		0.057	0.073	0.016		0.019	regulation of translation
Q16YE0	27	S	protein RCC2 homolog		0.367	0.588	0.412	0.395	0.022	
Q16WM9	694	S	extended synaptotagmin-2		0.013	0.357	0.357	0.008	0.024	lipid transport

five different time points spanning the entire process of vitellogenesis. The PCA analyses of our dataset (see Fig. 2A) shows that the biological replicates of specific time points PBM are strongly clustered giving confidence in the reproducibility of these phospho-peptide abundance data. Interestingly, the replicates of the unfed control group and the replicates of the 72-h PBM time point, were well separated. This indicates that the fat body does not fully return to its previtellogenic 'state of arrest' in which YPP expression is tightly repressed. This 'state of arrest' is rapidly terminated after a blood meal [38].

The results of the KEGG analyses of our dataset, that is shown in Figs. 3 and 4, confirms the notion that the regulation of mosquito vitellogenesis is a complex interplay between numerous cell-signaling pathways, many of which have already been implicated in this process. Earlier studies have clearly established that mTOR signaling, FoxO/insulin signaling, and autophagy are activated in mosquito females PBM [5,39–42]. In another study, it was observed that silencing of Notch in *Aedes aegypti* led to a 'sterile-like' phenotype that did not produce viable eggs [43]. Our results strongly suggest that the Notch signaling pathway is indeed active in the mosquito fat body after a blood meal.

The GO term analyses of our data set shown in Figs. 3 and 4, reveal cellular components and biological processes that highlight a hallmark of vitellogenesis-the rapid and massive synthesis of YPP's. In order to achieve this task, fat body trophocytes quadruple the number of ribosomes in their cytoplasm after a blood meal [44]. In accordance with this finding, we noticed high-fold enrichment of cellular component terms, that are the location of ribosome biogenesis. The enrichment of the term 'nucleolus' aligns with existing literature, as ribosome biogenesis takes place in this compartment [45,46]. We hypothesize, that the enrichment of the actin cyto-skeleton term may be linked to its function in transporting endosomal vesicles carrying YPPs to the cellular plasma membrane for secretion into the hemolymph [47].We found several pathways that were to our knowledge not previously implicated in the regulation of vitellogenesis in mosquitoes. Our data suggests, that the Hippo signaling pathway, a known regulator of cell proliferation and viral infection in mosquitoes [48,49], is active in the fat body during vitellogenesis. We also noted that the well-known immune pathway, Toll/IMD pathway [50], appeared in our analysis at the 24 and 48 h PBM time points, when yolk protein production by that fat body is at its peak. Another interesting finding is that the Spliceosome pathway [51] was enriched at each time point PBM. This suggests that at different time points PBM, specific mRNAs may be alternatively spliced. A thorough analysis of fat body transcriptome data could

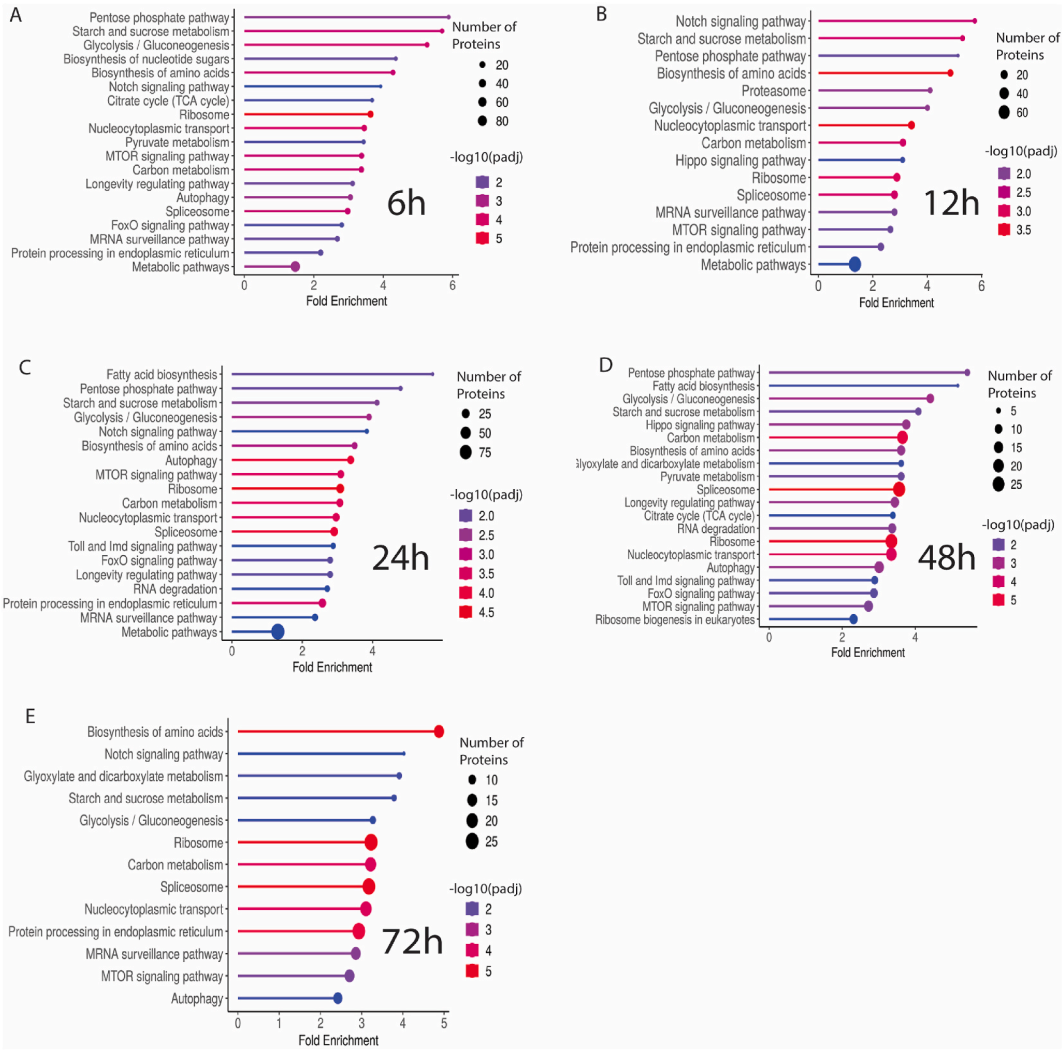

Fig. 4. KEGG pathway enrichment analyses by PBM time point. (A–E) Lollipop plots were generated using ShinyGO. Only significantly enriched pathways are shown (p-adjusted value using false discovery rate (FDR) < 0.05). Terms are sorted from top to bottom by fold enrichment, the percentage of proteins in each pathway divided by the percentage of genes in *Aedes aegypti* genome. The circles at the end of the lines represent the relative number of proteins identified in each pathway. The color of the line indicates the significance level. (A) 6h PBM; (B) 12h PBM; (C) 24h PBM; (D) 48h PBM; (E) 72h PBM.

identify such alternative splicing events in the future.

It is important to note that changes in phosphopeptide abundance can be explained by either a change in abundance of a parent protein, variation in the level of phosphorylation of a target phosphorylation site, or the combination of these factors [52] and a change in phosphorylation does not necessarily coincide with activation or deactivation, or in a change in enzyme activity of a protein [27]. Our top 10 list of phospho-peptides shown in Table 1, ranks phosphoproteins we observed with the highest and lowest fold-change at each time point PBM. Vitellogenin A1 is the only yolk protein precursor protein (YPP) present in these lists at all time points. As mentioned above, transcription and translation of YPPs is tightly repressed during the state-of-arrest before a blood meal and strongly up-regulated during vitellogenesis [14]. Therefore, we hypothesize that the high fold-change value we observed for this phospho-peptide is mainly due to the change in abundance of the parent protein during the process of vitellogenesis. We found nine phosphorylation sites within this protein, with a stretch of seven phosphoserine residues close to the C-terminus of the protein.

The other proteins in the top-ten lists (Table 1) fall into the categories of regulation of transcription, translation, posttranscriptional protein modification, signal transduction and metabolic processes which reflects the massive activation of YPP synthesis in this tissue.

In this study, for the first time, we identified 3570 phosphoproteins with 14,551 individual phosphorylation sites in *Ae. aegypti*. A limitation of our study is the fact that we used a single technique to generate our data. Confirmation of results for individual phosphoproteins will require the generation of phospho-specific antibodies, which is time-consuming and expensive. In future studies, we will use this approach to confirm our findings regarding the involvement of Notch and Hippo signaling pathways in the regulation of

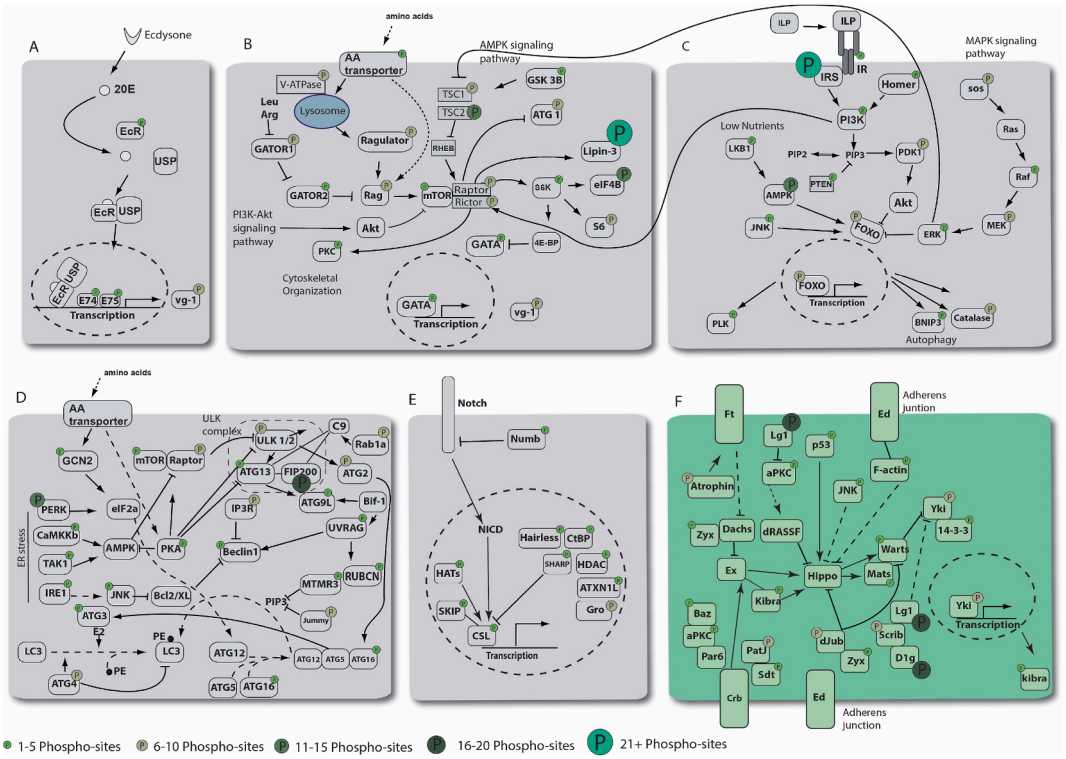

Fig. 5. Map of phospho-proteins in cellular signaling pathways that regulate YPP expression in mosquito fat body. Each large box represents a cell with proteins involved in specific signaling pathways. Grey boxes are pathways that have been previously identified as regulators of mosquito vitellogenesis, the green box marks the newly identified Hippo pathway. Small boxes within the cells represent proteins with abbreviated names. For full list of abbreviated proteins refer to Supplemental Tables 1–6. A green circle indicates that at least one phospho-site within the attached protein was identified in our dataset. The size of the green circle corresponds to the number of phospho-sites identified. The dotted circles represent a nucleus. Lines with an arrow represent activation, lines with a T-end represent repression. (A) Ecdysone signaling pathway-20E, 20 hydroxyecdysone; EcR, ecdysone receptor; USP, ultraspiracle; E74, Ecdysone-induced protein 74; E75, Ecdysone-induced protein 75; vg-1 vitellogenin 1. (B) mTOR signaling pathway. AA, amino acid. (C) FOXO signaling pathways. ILP, insulin-like peptide; IR, insulin receptor. (D) Autophagy signaling pathway. MTORC1, mechanistic target of rapamycin complex 1. (E) Notch signaling pathway. (F) Hippo signaling pathway.

mosquito vitellogenesis.

An interesting finding of the present study was that the majority of phosphopeptides detected in the fat body were significantly differentially abundant at each time point PBM compared to the unfed control. This is in contrast to our previous findings on the phosphoproteome of the Malpighian tubules of mosquitoes, where most phosphopeptides were not differentially abundant in unfed or fed mosquitoes [29].

Also, while some signaling pathways appear in both tissues, Malpighian tubules and fat bodies have clearly different phosphoproteomes, reflecting their different physiological roles.

In conclusion, we show that the blood-meal dependent activation of the mosquito fat body is a powerful model system to study nutrient signaling in a key metabolic organ. We describe a substantial number of novel phosphoproteins that change abundance in the course of mosquito vitellogenesis for the first time. We identified new leads that point towards novel nutrient-sensitive signaling pathways. Our work highlights the importance of post-translational protein modification in the post-embryonic development of mosquitoes and provides numerous leads for further studies into individual proteins involved in this process.

CRediT authorship contribution statement

April D. Lopez: Writing – original draft, Formal analysis, Conceptualization. **Tathagata Debnath:** Writing – review & editing, Visualization, Data curation, Conceptualization. **Matthew Pinch:** Writing – review & editing, Investigation, Conceptualization. **Immo A. Hansen:** Writing – review & editing, Writing – original draft, Investigation, Funding acquisition, Conceptualization.

Declaration of competing interest

All authors declare that they do not have competing interests regarding this study, neither financial nor otherwise.

Acknowledgments

The author's would like to thank Hailey Luker, Dela Esmaeili, Mahesh Lamsal, and Keyla Salas for technical assistance in this project. This research was funded by the National Institute of Health, grant number R35GM144049.

Appendix A. Supplementary data

Supplementary data to this article can be found online at https://doi.org/10.1016/j.heliyon.2024.e40060.

References

[1] H. Dahmana, O. Mediannikov, Mosquito-borne diseases emergence/resurgence and how to effectively control it biologically, Pathogens 9 (2020).
[2] P. Wu, X. Yu, P. Wang, G. Cheng, Arbovirus lifecycle in mosquito: acquisition, propagation and transmission, Expert Rev Mol Med 21 (2019) e1.
[3] D.Y. Boudko, H. Tsujimoto, S.D. Rodriguez, E.A. Meleshkevitch, D.P. Price, L.L. Drake, I.A. Hansen, Substrate specificity and transport mechanism of amino-acid transceptor Slimfast from Aedes aegypti, Nat. Commun. 6 (2015) 8546.
[4] I.A. Hansen, G.M. Attardo, Nutritional signaling in anautogenous mosquitoes, in: R. Chandrasekar (Ed.), Short Views on Insect Molecular Biology, International Book Mission, South India), 2009.
[5] I.A. Hansen, G.M. Attardo, S.D. Rodriguez, L.L. Drake, Four-way regulation of mosquito yolk protein precursor genes by juvenile hormone-, ecdysone-, nutrient-, and insulin-like peptide signaling pathways, Front. Physiol. 5 (2014) 103.
[6] M. Pinch, S. Mitra, S.D. Rodriguez, Y. Li, Y. Kandel, B. Dungan, F.O. Holguin, G.M. Attardo, I.A. Hansen, Fat and happy: profiling mosquito fat body lipid storage and composition post-blood meal, Frontiers in Insect Science 1 (2021) 6.
[7] D.P. Price, V. Nagarajan, A. Churbanov, P. Houde, B. Milligan, L.L. Drake, J.E. Gustafson, I.A. Hansen, The fat body transcriptomes of the yellow fever mosquito Aedes aegypti, pre- and post- blood meal, PLoS One 6 (2011) e22573.
[8] P. Skowronek, Ł. Wójcik, A. Strachecka, Fat body-multifunctional insect tissue, Insects 12 (2021).
[9] I.A. Hansen, S.R. Meyer, I. Schafer, K. Scheller, Interaction of the anterior fat body protein with the hexamerin receptor in the blowfly Calliphora vicina, Eur. J. Biochem. 269 (2002) 954–960.
[10] H.-N. Chung, S.D. Rodriguez, V.K. Carpenter, J. Vulcan, C.D. Bailey, M. Nageswara-Rao, Y. Li, G.M. Attardo, I.A. Hansen, Fat body organ culture system in Aedes aegypti, a vector of zika virus, J. Vis. Exp. 126 (2017) e55508.
[11] M. Pinch, S. Mitra, S.D. Rodriguez, Y. Li, Y. Kandel, B. Dungan, F.O. Holguin, G.M. Attardo, I.A. Hansen, Fat and happy: profiling mosquito fat body lipid storage and composition post-blood meal, Frontiers in Insect Science 1 (2021).
[12] G.F. Martins, J.E. Serrão, J.M. Ramalho-Ortigão, P.F. Pimenta, A comparative study of fat body morphology in five mosquito species, Mem. Inst. Oswaldo Cruz 106 (2011) 742–747.
[13] D.P. Price, F.D. Schilkey, A. Ulanov, I.A. Hansen, Small mosquitoes, large implications: crowding and starvation affects gene expression and nutrient accumulation in Aedes aegypti, Parasit Vectors 8 (2015) 252.
[14] D.P. Price, V. Nagarajan, A. Churbanov, P. Houde, B. Milligan, L.L. Drake, J.E. Gustafson, I.A. Hansen, The fat body transcriptomes of the yellow fever mosquito Aedes aegypti, pre- and post- blood meal, PLoS One 6 (2011).
[15] Q. Yang, J. Zhao, D. Chen, Y. Wang, E3 ubiquitin ligases: styles, structures and functions, Mol Biomed 2 (2021) 23.
[16] Z. Wu, L. Yang, Q. He, S. Zhou, Regulatory mechanisms of vitellogenesis in insects, Front. Cell Dev. Biol. 8 (2020) 593613.
[17] A.S. Raikhel, V.A. Kokoza, J. Zhu, D. Martin, S.F. Wang, C. Li, G. Sun, A. Ahmed, N. Dittmer, G. Attardo, Molecular biology of mosquito vitellogenesis: from basic studies to genetic engineering of antipathogen immunity, Insect Biochem. Mol. Biol. 32 (2002) 1275–1286.
[18] S. Roy, T.T. Saha, Z. Zou, A.S. Raikhel, Regulatory pathways controlling female insect reproduction, Annu. Rev. Entomol. 63 (2018) 489–511.
[19] L. Valzania, M.T. Mattee, M.R. Strand, M.R. Brown, Blood feeding activates the vitellogenic stage of oogenesis in the mosquito Aedes aegypti through inhibition of glycogen synthase kinase 3 by the insulin and TOR pathways, Dev. Biol. 454 (2019) 85–95.
[20] Z. Wu, L. Yang, Q. He, S. Zhou, Regulatory mechanisms of vitellogenesis in insects, Front. Cell Dev. Biol. 8 (2021).
[21] A. Baker, C.C. Lin, C. Lett, B. Karpinska, M.H. Wright, C.H. Foyer, Catalase: a critical node in the regulation of cell fate, Free Radic. Biol. Med. 199 (2023) 56–66.
[22] S.H. Shiao, I.A. Hansen, J. Zhu, D.H. Sieglaff, A.S. Raikhel, Juvenile hormone connects larval nutrition with target of rapamycin signaling in the mosquito Aedes aegypti, J. Insect Physiol. 54 (2008) 231–239.
[23] H. Gujar, S.R. Palli, Juvenile hormone regulation of female reproduction in the common bed bug, Cimex lectularius, Sci. Rep. 6 (2016) 35546.
[24] L. Ling, A.S. Raikhel, Amino acid-dependent regulation of insulin-like peptide signaling is mediated by TOR and GATA factors in the disease vector mosquito Aedes aegypti, Proc Natl Acad Sci U S A 120 (2023) e2303234120.
[25] I.A. Hansen, D.H. Sieglaff, J.B. Munro, S.H. Shiao, J. Cruz, I.W. Lee, J.M. Heraty, A.S. Raikhel, Forkhead transcription factors regulate mosquito reproduction, Insect Biochem. Mol. Biol. 37 (2007) 985–997.
[26] J.S. Gerritsen, F.M. White, Phosphoproteomics: a valuable tool for uncovering molecular signaling in cancer cells, Expert Rev. Proteomics 18 (2021) 661–674.
[27] F. Ardito, M. Giuliani, D. Perrone, G. Troiano, L. Lo Muzio, The crucial role of protein phosphorylation in cell signaling and its use as targeted therapy, Int. J. Mol. Med. 40 (2017) 271–280.
[28] S. Morandell, T. Stasyk, K. Grosstessner-Hain, E. Roitinger, K. Mechtler, G.K. Bonn, L.A. Huber, Phosphoproteomics strategies for the functional analysis of signal transduction, Proteomics 6 (2006) 4047–4056.
[29] Y. Kandel, M. Pinch, M. Lamsal, N. Martinez, I.A. Hansen, Exploratory phosphoproteomics profiling of Aedes aegypti Malpighian tubules during blood meal processing reveals dramatic transition in function, PLoS One 17 (2022) e0271248.
[30] Chapter 2 - general biology of salmonids, Dev. Aquacult. Fish. Sci. 29 (1996) 29–95.
[31] H.-N. Au - Chung, S.D. Au - Rodriguez, V.K. Au - Carpenter, J. Au - Vulcan, C.D. Au - Bailey, M. Au - Nageswara-Rao, Y. Au - Li, G.M. Au - Attardo, I.A. Au - Hansen, Fat body organ culture system in Aedes aegypti, a vector of zika virus, JoVE (2017) e55508.
[32] E. Elhaik, Principal Component Analyses (PCA)-based findings in population genetic studies are highly biased and must be reevaluated, Sci. Rep. 12 (2022) 14683.
[33] S.X. Ge, D. Jung, R. Yao, ShinyGO: a graphical gene-set enrichment tool for animals and plants, Bioinformatics 36 (2019) 2628–2629.
[34] M. Pinch, T. Muka, Y. Kandel, M. Lamsal, N. Martinez, M. Teixeira, D.Y. Boudko, I.A. Hansen, General control nonderepressible 1 interacts with cationic amino acid transporter 1 and affects Aedes aegypti fecundity, Parasites Vectors 15 (2022) 1–17.
[35] A.C. Vind, G. Snieckute, S. Bekker-Jensen, M. Blasius, Ribosome Run, Run: from compromised translation to human health, Antioxidants Redox Signal ing 39 (2023) 4–6.
[36] G.M. Attardo, I.A. Hansen, S.H. Shiao, A.S. Raikhel, Identification of two cationic amino acid transporters required for nutritional signaling during mosquito reproduction, J. Exp. Biol. 209 (2006) 3071–3078.
[37] H. Zhang, F.G. Goh, L.C. Ng, C.H. Chen, Y. Cai, Aedes aegypti exhibits a distinctive mode of late ovarian development, BMC Biol. 21 (2023) 11.

[38] J. Dittmer, A. Alafndi, P. Gabrieli, Fat body–specific vitellogenin expression regulates host-seeking behaviour in the mosquito Aedes albopictus, PLoS Biol. 17 (2019) e3000238.
[39] I.A. Hansen, G.M. Attardo, S.G. Roy, A.S. Raikhel, Target of rapamycin-dependent activation of S6 kinase is a central step in the transduction of nutritional signals during egg development in a mosquito, J. Biol. Chem. 280 (2005) 20565–20572.
[40] L. Ling, A.S. Raikhel, Cross-talk of insulin-like peptides, juvenile hormone, and 20-hydroxyecdysone in regulation of metabolism in the mosquito Aedes aegypti, Proc. Natl. Acad. Sci. USA 118 (2021) e2023470118.
[41] S.G. Roy, I.A. Hansen, A.S. Raikhel, Effect of insulin and 20-hydroxyecdysone in the fat body of the yellow fever mosquito, Aedes aegypti, Insect Biochem. Mol. Biol. 37 (2007) 1317–1326.
[42] B. Bryant, A.S. Raikhel, Programmed autophagy in the fat body of Aedes aegypti is required to maintain egg maturation cycles, PLoS One 6 (2011) e25502.
[43] C.H. Chang, Y.T. Liu, S.C. Weng, I.Y. Chen, P.N. Tsao, S.H. Shiao, The non-canonical Notch signaling is essential for the control of fertility in Aedes aegypti, PLoS Negl Trop Dis 12 (2018) e0006307.
[44] P.G. Hotchkin, A.M. Fallo, Ribosome metabolism during the vitellogenic cycle of the mosquito, Aedes aegypti, Biochimica et Biophysica Acta (BBA)-General Subjects 924 (1987) 352–359.
[45] D.L. Lafontaine, D. Tollervey, The function and synthesis of ribosomes, Nat. Rev. Mol. Cell Biol. 2 (2001) 514–520.
[46] A.C. Vind, G. Snieckute, S. Bekker-Jensen, M. Blasius, Run, ribosome, run: from compromised translation to human health, Antioxidants Redox Signal. 39 (2023) 336–350.
[47] W. Wang, R.-R. Yang, L.-Y. Peng, L. Zhang, Y.-L. Yao, Y.-Y. Bao, Proteolytic activity of the proteasome is required for female insect reproduction, Open Biology 11 (2021) 200251.
[48] M.-j. Li, C.-j. Lan, H.-t. Gao, D. Xing, Z.-y. Gu, D. Su, T.-y. Zhao, H.-y. Yang, C.-x. Li, Transcriptome analysis of Aedes aegypti Aag2 cells in response to dengue virus-2 infection, Parasites Vectors 13 (2020) 1–14.
[49] D. Pan, The unfolding of the Hippo signaling pathway, Developmental biology 487 (2022) 1–9.
[50] J.L. Ramirez, E.J. Muturi, A.B. Barletta, A.P. Rooney, The Aedes aegypti IMD pathway is a critical component of the mosquito antifungal immune response, Dev. Comp. Immunol. 95 (2019) 1–9.
[51] C.L. Will, R. Lührmann, Spliceosome structure and function, Cold Spring Harbor Perspect. Biol. 3 (2011) a003707.
[52] T. Zhang, G.R. Keele, I.G. Gyuricza, M. Vincent, C. Brunton, T.A. Bell, P. Hock, G.D. Shaw, S.C. Munger, F.P.-M. de Villena, Multi-omics analysis identifies drivers of protein phosphorylation, Genome biology 24 (2023) 52.